

An Accurate Total Energy Density Functional

BAOJING ZHOU, YAN ALEXANDER WANG

Department of Chemistry, University of British Columbia, Vancouver, BC Canada V6T 1Z1

Received 27 February 2007; accepted 29 May 2007

Published online 31 July 2007 in Wiley InterScience (www.interscience.wiley.com).

DOI 10.1002/qua.21471

ABSTRACT: We propose a new density functional for the evaluation of the total electronic energy by subtracting the Roothaan energy, i.e. the Hartree energy of the density residual, from the Hohenberg–Kohn–Sham (HKS) functional, which is normally used in self-consistent Kohn–Sham (KS) density functional theory (DFT) calculations. Because of the positive semi-definite nature of the Roothaan energy, the resulting Wang–Zhou (WZ) functional always produces a total energy lower than that from the HKS functional and usually converges to the exact total energy from below. Following the same spirit of the Zhou–Wang- λ (ZW λ) functional in the recently proposed orbital-corrected orbital-free (OO) DFT method (Zhou and Wang, *J Chem Phys* 2006, 124, 081107), we linearly mix the WZ functional with the HKS functional to allow further systematic error cancellations. The resulting Wang–Zhou- α (WZ α) functional is compared with the ZW λ functional in OO-DFT calculations for systems within different chemical environment. We find that the optimal value of α for the WZ α functional is more stable than that of λ for the ZW λ functional. This is because the WZ functional remedies the oscillatory convergence behavior of the Harris functional and renders the direct evaluation of α for the WZ α functional more plausible in the application of the linear-scaling OO-DFT method for large systems. © 2007 Wiley Periodicals, Inc. *Int J Quantum Chem* 107: 2995–3000, 2007

Key words: Kohn–Sham; orbital free; density functional; total energy; Harris functional

Density functional theory (DFT) [1], one of the most widely used first-principles quantum mechanics methods, provides an approximate yet rigorous approach to treat the many-body problem of N interacting electrons and plays a vital role in understanding the properties of matter. However, its

general large-scale applications are still confronted with difficulties. Its two most common implementations, the orbital-based Kohn–Sham (KS) DFT [2] and orbital-free (OF) DFT [3], have their own strengths and weaknesses.

In KS-DFT, the following KS equations (in Hartree atomic units) are solved:

$$\left(-\frac{1}{2}\nabla^2 + v_{\text{eff}}^{\text{KS}}[\rho](\mathbf{r})\right)\phi_i(\mathbf{r}) = \epsilon_i\phi_i(\mathbf{r}), \quad (1)$$

Correspondence to: Y.A. Wang; e-mail: yawang@chem.ubc.ca
Contract grant sponsors: Natural Sciences and Engineering Research Council of Canada.

where the KS effective potential, $v_{\text{eff}}^{\text{KS}}[\rho](\mathbf{r})$, contains the Hartree, exchange-correlation (XC), and ion–electron potentials:

$$\begin{aligned} v_{\text{eff}}^{\text{KS}}[\rho](\mathbf{r}) &= \frac{\delta E_{\text{H}}[\rho]}{\delta \rho(\mathbf{r})} + \frac{\delta E_{\text{xc}}[\rho]}{\delta \rho(\mathbf{r})} + v_{\text{ne}}(\mathbf{r}) \\ &= v_{\text{H}}[\rho](\mathbf{r}) + v_{\text{xc}}[\rho](\mathbf{r}) + v_{\text{ne}}(\mathbf{r}). \end{aligned} \quad (2)$$

With the iterative methods [4], the KS effective potential constructed from some input density, $v_{\text{eff}}^{\text{KS}}[\rho_{\text{in}}]$, is fixed at each iteration, and the new density is obtained from the output orbitals:

$$\rho_{\text{out}}(\mathbf{r}) = \sum_i f_i |\phi_i(\mathbf{r})|^2, \quad (3)$$

where f_i is the occupation number of the i th KS orbital ϕ_i . Working in a plane-wave basis set, we can take advantage of some density mixing schemes [4] to generate the input density for the next iteration in reciprocal space:

$$\rho_{\text{in}}^{i+1} = \rho_{\text{in}}^i + \mathbf{G}R[\rho_{\text{in}}^i], \quad (4)$$

where \mathbf{G} is the preconditioning matrix to reduce the density residual $R[\rho_{\text{in}}]$,

$$R[\rho_{\text{in}}] = \rho_{\text{out}} - \rho_{\text{in}}. \quad (5)$$

In different density mixing schemes, \mathbf{G} takes different forms [4]. The simplest preconditioning matrix is just a unit matrix multiplied by a constant, which corresponds to linear mixing. In the well-known Kerker scheme [5], the preconditioning matrix is diagonal in reciprocal space and takes the following form for the reciprocal space wave vector [6], q ,

$$\mathbf{G}(q) = A \frac{q}{q^2 + q_0^2}, \quad (6)$$

where A and q_0 are two parameters. In more robust, sophisticated density mixing schemes, such as the Pulay scheme [7], the preconditioning matrix can have non-zero off-diagonal elements in reciprocal space [4].

For each iteration, the Hohenberg–Kohn–Sham (HKS) functional [8] is usually employed to evaluate the total electronic energy:

$$\begin{aligned} E^{\text{HKS}}[\rho_{\text{in}}, \rho_{\text{out}}] &= \sum_i f_i \epsilon_i + E_{\text{H}}[\rho_{\text{out}}] - \langle \rho_{\text{out}}(\mathbf{r}) v_{\text{H}}[\rho_{\text{in}}] \rangle \\ &\quad + E_{\text{xc}}[\rho_{\text{out}}] - \langle \rho_{\text{out}}(\mathbf{r}) v_{\text{xc}}[\rho_{\text{in}}] \rangle. \end{aligned} \quad (7)$$

Upon the full self consistency, the converged KS orbitals of Eq. (1) yield the exact KS density, $\rho_{\text{KS}}(\mathbf{r})$, and the HKS functional becomes the exact total KS electronic energy, E^{KS} ,

$$\begin{aligned} E^{\text{KS}}[\rho_{\text{KS}}] &= \sum_i f_i \left\langle \phi_i \left| -\frac{1}{2} \nabla^2 \right| \phi_i \right\rangle + E_{\text{H}}[\rho_{\text{KS}}] \\ &\quad + E_{\text{xc}}[\rho_{\text{KS}}] + \langle \rho_{\text{KS}}(\mathbf{r}) v_{\text{ne}}(\mathbf{r}) \rangle. \end{aligned} \quad (8)$$

In the conventional KS-DFT method, the cost of each iteration scales as $\mathcal{O}(N^3)$ due to the orbital orthonormalization. Although many linear-scaling algorithms [9] developed in the last decade allow the computational cost increases linearly with the size of the system, the total cost is still quite high because a large number of iterations are needed to reach self consistency [4]. To avoid the many iterations in self-consistent KS-DFT calculations, the Harris functional [10] is often used for a fast yet accurate evaluation of the total electronic energy:

$$\begin{aligned} E^{\text{Harris}}[\rho_{\text{in}}, \rho_{\text{out}}] &= \sum_i f_i \epsilon_i - E_{\text{H}}[\rho_{\text{in}}] + E_{\text{xc}}[\rho_{\text{in}}] \\ &\quad - \langle \rho_{\text{in}}(\mathbf{r}) v_{\text{xc}}[\rho_{\text{in}}] \rangle, \end{aligned} \quad (9)$$

when a good approximation to the exact KS density is available [11–13]. However, the Harris functional is not necessarily more accurate than the HKS functional and can be either a saddle point or a local minimum at the exact KS density [12]. Consequently, the error of the Harris functional can be either positive or negative, as will be shown later.

On the other hand, OF-DFT can be implemented essentially as a linear-scaling method with computational cost of $\mathcal{O}(N \ln N)$ [3]. Currently, OF-DFT calculations have not achieved high accuracy consistently, mainly because of the lack of an accurate kinetic energy density functional (KEDF) [3] and high-quality local pseudopotentials (LPS) [14]. The recently proposed orbital-corrected OF-DFT (OO-DFT) [15], a new implementation of DFT, retains the merits of both KS-DFT and OF-DFT and avoids their drawbacks. The special features of OO-DFT lie in two aspects: (i) the high-quality density generated from OF-DFT is used as the initial input density for subsequent KS-DFT calculations and (ii) the Zhou–Wang- λ (ZW λ) functional is used to evaluate the

total electronic energy,

$$E^{\text{ZW}\lambda}[\rho_{\text{in}}, \rho_{\text{out}}] = (1 - \lambda)E^{\text{HKS}}[\rho_{\text{in}}, \rho_{\text{out}}] + \lambda E^{\text{Harris}}[\rho_{\text{in}}, \rho_{\text{out}}], \quad (10)$$

where λ is an interpolation parameter. The form of the $\text{ZW}\lambda$ functional can be rationalized by the analysis on the following second-order errors in the HKS and Harris functionals with respect to the exact KS energy [13]:

$$E^{\text{HKS}} - E^{\text{KS}} = \langle R[\rho_{\text{in}}(\mathbf{r})]C(\mathbf{r}, \mathbf{r}')[\rho_{\text{out}}(\mathbf{r}') - \rho_{\text{KS}}(\mathbf{r}')] \rangle + O(\delta\rho^3), \quad (11)$$

$$E^{\text{Harris}} - E^{\text{KS}} = \langle R[\rho_{\text{in}}(\mathbf{r})]C(\mathbf{r}, \mathbf{r}')[\rho_{\text{in}}(\mathbf{r}') - \rho_{\text{KS}}(\mathbf{r}')] \rangle + O(\delta\rho^3), \quad (12)$$

where $C(\mathbf{r}, \mathbf{r}')$ is given by

$$C(\mathbf{r}, \mathbf{r}') = \frac{1}{2} \left(\frac{1}{|\mathbf{r} - \mathbf{r}'|} + \left. \frac{\delta v_{\text{xc}}[\rho](\mathbf{r})}{\delta\rho(\mathbf{r}')} \right|_{\rho_{\text{in}}} \right). \quad (13)$$

In our previous work [15], we found that for simple bulk systems, such as the cubic diamond (CD) Si and the face-centered-cubic (fcc) Ag, a linear combination of $\rho_{\text{in}}(\mathbf{r})$ and $\rho_{\text{out}}(\mathbf{r})$ usually provides a good approximation to $\rho_{\text{KS}}(\mathbf{r})$,

$$\rho_{\text{KS}}(\mathbf{r}) \approx (1 - \lambda)\rho_{\text{out}}(\mathbf{r}) + \lambda\rho_{\text{in}}(\mathbf{r}), \quad (14)$$

and the mixing parameter, λ , closely mimic the reciprocal space density mixing parameters at the first one or two Bragg vectors [6]. A close inspection of Eqs. (11)–(14) reveals that the second-order errors in the HKS and Harris functionals can be systematically canceled by the $\text{ZW}\lambda$ functional in Eq. (10). For complex systems, Eq. (14) is less likely to be a good approximation; however, one still expects some systematic error cancelations to occur in the $\text{ZW}\lambda$ functional with an appropriate λ .

The performance of the $\text{ZW}\lambda$ functional has been demonstrated in our previous OO-DFT calculations on the CD Si and the fcc Ag systems [15]. During more extensive tests of the $\text{ZW}\lambda$ functional, we found that its optimal λ value fluctuates a lot from iteration to iteration, sometimes out of the range from 0 to 1. This undesirable feature is mainly due to the oscillatory convergence behavior of the Harris functional and causes difficulty in a direct evaluation for the

optimal value of λ . To remedy this defect, we subtract the Roothaan energy [16, 17],

$$E^{\text{R}}[\rho_{\text{in}}, \rho_{\text{out}}] = \frac{1}{2} \left\langle \frac{R[\rho_{\text{in}}(\mathbf{r})]R[\rho_{\text{in}}(\mathbf{r}')]}{|\mathbf{r} - \mathbf{r}'|} \right\rangle, \quad (15)$$

from the HKS functional to obtain the Wang–Zhou (WZ) functional:

$$E^{\text{WZ}}[\rho_{\text{in}}, \rho_{\text{out}}] = E^{\text{HKS}}[\rho_{\text{in}}, \rho_{\text{out}}] - E^{\text{R}}[\rho_{\text{in}}, \rho_{\text{out}}] = \sum_i f_i \epsilon_i - E_{\text{H}}[\rho_{\text{in}}] + E_{\text{xc}}[\rho_{\text{out}}] - \langle \rho_{\text{out}}(\mathbf{r})v_{\text{xc}}[\rho_{\text{in}}] \rangle. \quad (16)$$

Here, the first and the last two terms on the right-hand side of the second equal sign are identical to the first two terms in the Harris functional [Eq. (9)] and the last two terms in the HKS functional [Eq. (7)], respectively. Note that the Roothaan energy is a positive semi-definite quantity [16, 17] and it smoothly converges to 0 as the density residual vanishes [18]. Thus, the WZ functional always produces a lower total energy than the HKS functional does, and the oscillatory convergence behavior exhibited in the Harris functional is completely eliminated. Later, we will see that E^{WZ} usually converges to E^{KS} from below; however, whether it is a lower bound to E^{KS} remains to be proven.

Based on Eqs. (11) and (16), the second-order errors in the WZ functional have two contributions:

$$E^{\text{WZ}} - E^{\text{KS}} = \frac{1}{2} \left\langle R[\rho_{\text{in}}(\mathbf{r})] \left(\left. \frac{\delta v_{\text{xc}}[\rho](\mathbf{r})}{\delta\rho(\mathbf{r}')} \right|_{\rho_{\text{in}}} \right) [\rho_{\text{out}}(\mathbf{r}') - \rho_{\text{KS}}(\mathbf{r}')] \right\rangle + \frac{1}{2} \left\langle \frac{R[\rho_{\text{in}}(\mathbf{r})]}{|\mathbf{r} - \mathbf{r}'|} [\rho_{\text{in}}(\mathbf{r}') - \rho_{\text{KS}}(\mathbf{r}')] \right\rangle + O(\delta\rho^3). \quad (17)$$

To allow further error cancelations between E^{HKS} and E^{WZ} , we again linearly mix the WZ functional with the HKS functional, resulting in the Wang–Zhou- α ($\text{WZ}\alpha$) functional,

$$E^{\text{WZ}\alpha}[\rho_{\text{in}}, \rho_{\text{out}}] = (1 - \alpha)E^{\text{HKS}}[\rho_{\text{in}}, \rho_{\text{out}}] + \alpha E^{\text{WZ}}[\rho_{\text{in}}, \rho_{\text{out}}] = E^{\text{HKS}}[\rho_{\text{in}}, \rho_{\text{out}}] - \alpha E^{\text{R}}[\rho_{\text{in}}, \rho_{\text{out}}], \quad (18)$$

with the mixing parameter α . Eq. (18) shall cancel the errors of the terms involving $\frac{1}{|\mathbf{r} - \mathbf{r}'|}$ in Eqs. (11)

and (17), if Eq. (14) provides a good approximation with the optimal value of α . In essence, the $WZ\alpha$ functional utilizes part of the Roothaan energy to cancel the error in the HKS functional. Interestingly, employing the existing code of computing the Hartree energy for the evaluation of the Roothaan energy enables the $WZ\alpha$ functional to be used not only in DFT methods but also in other first-principles methods utilizing self-consistent iterations. The cost of computing the Roothaan energy only increases linearly with the size of the system even when strictly confined basis orbitals are employed [19].

We test the WZ and $WZ\alpha$ functionals in OO-DFT calculations on the following systems: the CD Si, the fcc Ag, and the CD Si vacancy and (100) surface. Orthorhombic unit cells containing 8 and 4 atoms are used for the CD Si and the fcc Ag, respectively. A $2 \times 2 \times 2$ super cell containing 63 atoms and 1 vacancy is used for the CD Si vacancy. The CD Si (100) surface contains a five-layer slab with two atoms per layer and the vacuum has the same dimension as the slab. The local density approximation (LDA) [20] is used in all DFT calculations.

For the CD Si and the fcc Ag, all DFT calculations are carried out under the same conditions as those in Ref. 15. For the CD Si vacancy and (100) surface, the kinetic-energy cutoffs for the plane-wave basis set are chosen to be 760 eV for OO-DFT and KS-DFT calculations and 1.52 KeV for OF-DFT calculations to ensure all the computed quantities are fully converged with respect to the basis set. The Wang-Govind-Carter (WGC) [21] KEDF and the LPS

derived from a bulk environment [14] are employed in OF-DFT calculations. A modified *ABINIT* code [22] is used to run OO-DFT and KS-DFT calculations, in which the standard Troullier-Martins nonlocal pseudopotentials (NLPS) [23] are employed. For the CD Si vacancy, we find that it is adequate to only employ the Γ point for the Brillouin-zone (BZ) sampling [6]. For the CD Si (100) surface, a $6 \times 6 \times 1$ Monkhorst-Pack grid [24] with 28 irreducible \mathbf{k} -points is used for the BZ sampling. In OO-DFT calculations on the CD Si vacancy and (100) surface, we adopt Kerker's formula [5] [see Eq. (6)] for the preconditioning matrix at the end of the first iteration, with the recommended values [4] for the two parameters: $A = 0.8$, and $q_0 = 1.5 \text{ \AA}^{-1}$. For the subsequent iterations, the Pulay's scheme [7] is employed for density mixing.

The total energies of the CD Si at different cell volumes are evaluated from the HKS, WZ , and $WZ\alpha$ functionals with the densities from the first iteration in OO-DFT and are compared with the fully converged KS results in Figure 1(a). The HKS functional slightly overestimates the total energies at relatively large cell volumes, whereas the WZ functional significantly underestimates them. With $\alpha = 0.16$, the $WZ\alpha$ functional is able to reproduce the fully converged KS energies accurately.

Figure 1(b) depicts the total energies of the fcc Ag at different cell volumes using the HKS, WZ , and $WZ\alpha$ functionals in OO-DFT. The results from the first iteration are shown in the inset: both the HKS and WZ functionals lead to large errors at relatively

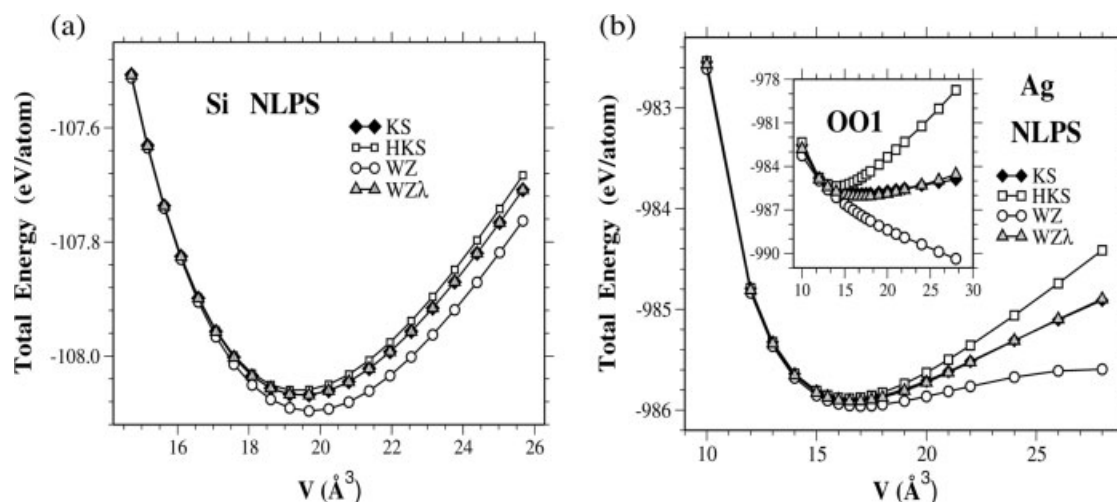


FIGURE 1. LDA total energies (in eV/atom) versus cell volume V (in \AA^3) for (a) the CD Si and (b) the fcc Ag. The results from the HKS (open square), WZ (open circle), and $WZ\alpha$ (opaque triangle) functionals in OO-DFT are compared with those from KS-DFT (solid diamond).

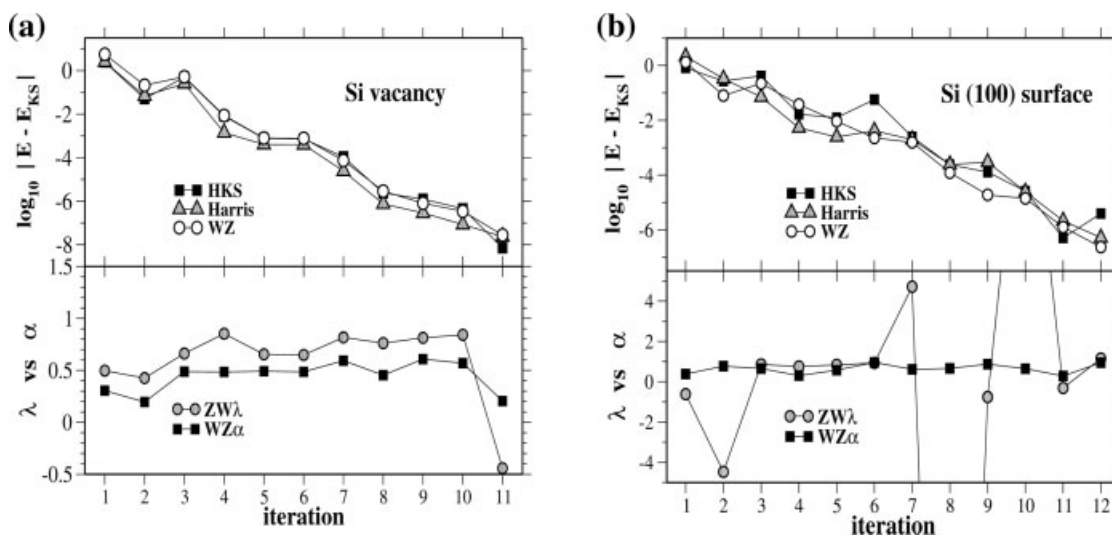


FIGURE 2. Convergence of total energies (in eV) evaluated from the HKS (solid square), Harris (opaque triangles), and WZ (open circles) functionals (top panels) and the optimal λ value of the $ZW\lambda$ (opaque circles) functional vs. the optimal α value of the $WZ\alpha$ (solid square) functional (bottom panels) during the self-consistent iterations for (a) the CD Si vacancy and (b) the CD Si (100) surface systems. In the lower panel of (b), the optimal values of λ are -46.25 and 16.97 at iterations 8 and 10, respectively.

large cell volumes, and the $WZ\alpha$ functional yields much better results with $\alpha = 0.50$. At the second iteration, the input density is chosen to be the average of the input and output densities from the first iteration. We see that errors in the HKS and WZ functionals are significantly suppressed, though visible deviations from the KS results still exist at relatively large cell volumes. With $\alpha = 0.41$, the total energies from the $WZ\alpha$ functional almost exactly match those KS results.

The total energies of the CD Si vacancy and (100) surface are computed in OO-DFT from the HKS, Harris, and WZ functionals. The top panels of Figure 2 illustrate the convergence behavior of those functionals. For the CD Si vacancy [top panel of Fig. 2(a)], the Harris functional is usually more accurate than the HKS and WZ functionals. Consequently, the optimal λ of the $ZW\lambda$ functional is usually larger than 0.5 as shown in the bottom panel of Figure 2(a). In contrast, the optimal α value of the $WZ\alpha$ functional is around 0.5 because the absolute error in the WZ functional is about the same as that in the HKS functional [see the top panel of Fig. 2(a)]. Note that the optimal λ value of the $ZW\lambda$ functional becomes negative at the eleventh iteration when $E^{KS} < E^{HKS} < E^{Harris}$. On the other hand, the optimal α value of the $WZ\alpha$ functional is always between 0 and 1, reflecting that the WZ functional yields a total energy lower than the exact KS energy.

The advantage of the $WZ\alpha$ functional over the $ZW\lambda$ functional is more obvious in OO-DFT calculations on the more complex CD Si (100) surface system. From the top panel of Figure 2(b), we see that the Harris functional is not necessarily more accurate than the HKS and WZ functionals. Moreover, the convergence patterns of the HKS, Harris, and WZ functionals are clearly different from one another. As seen from the bottom panel of Fig. 2(b), the optimal λ value of the $ZW\lambda$ functional fluctuates much more drastically than that for the CD Si vacancy system. At the first, second, eighth, ninth, and eleventh iterations when $E^{KS} < E^{HKS} < E^{Harris}$, the optimal λ value is negative; while at the seventh, tenth, and twelfth iterations when $E^{KS} < E^{Harris} < E^{HKS}$, the optimal λ value is above 1. This poses a great difficulty in direct evaluation of the λ value for the $ZW\lambda$ functional. In comparison, the fluctuation of the optimal α value is strongly suppressed in the $WZ\alpha$ functional.

Lifting the requirement for the full self-consistency, the use of the $WZ\alpha$ functional in OO-DFT or other iterative first-principles methods is expected to significantly lower the computational cost if the optimal value for the mixing parameter α of the $WZ\alpha$ functional can be readily determined. One simple solution is to find the optimal α value for a small subsystem whose chemical environment closely mimics that of the entire big system and to use the same

α value in subsequent OO-DFT calculations for the entire system. More attractively, the optimal α value can be directly evaluated from the density mixing parameters on the fly. We are currently working along this direction.

In conclusion, we have designed a new total energy density functional, i.e., the WZ functional, which usually converges to the exact KS energy from below and remedies the defect of the Harris functional. The $WZ\alpha$ functional, a linear combination of the HKS and WZ functionals, allows further error cancellations and its accuracy is demonstrated by OO-DFT calculations on systems within different chemical environment. Compared with the $ZW\lambda$ functional proposed in our earlier work [15], the $WZ\alpha$ functional can accurately reproduce the fully converged KS energy with much more consistent, stable optimal α value.

ACKNOWLEDGMENT

Financial support for this project was provided by a grant from the Natural Sciences and Engineering Research Council of Canada.

References

- Hohenberg, P.; Kohn, W. *Phys Rev* 1964, 136, B864.
- Kohn, W.; Sham, L. J. *Phys Rev* 1965, 140, A1133.
- Wang, Y. A.; Carter, E. A. In *Theoretical Methods in Condensed Phase Chemistry*; Schwartz, S. D., Eds.; Kluwer: Dordrecht, 2000; p 117.
- Kresse, G.; Furthmüller, J. *Comput Mater Sci* 1996, 6, 15.
- Kerker, G. P. *Phys Rev B* 1981, 23, 3082.
- Ashcroft, N. W.; Mermin, N. D. *Solid State Physics*; Saunders: Orlando, 1976.
- Pulay, P. *Chem Phys Lett* 1980, 73, 393.
- Chelikowsky, J. R.; Louie, S. G. *Phys Rev B* 1984, 29, 3470.
- (a) Goedecker, S. *Rev Mod Phys* 1999, 71, 1085; (b) Kohn, W. *Phys Rev Lett* 1996, 76, 3168.
- Harris, J. *Phys Rev B* 1985, 31, 1770.
- (a) Polatoglou, H. M.; Methfessel, M. *Phys Rev B* 1988, 37, 10403; (b) Read, A. J.; Needs, R. J. *J Phys Condens Matter* 1989, 1, 7565.
- (a) Robertson, I. J.; Farid, B. *Phys Rev Lett* 1991, 66, 3265; (b) Zaremba, E. *J Phys Condens Matter* 1990, 2, 2479.
- Finnis, M. W. *J Phys Condens Matter* 1990, 2, 331.
- Zhou, B.; Wang, Y. A.; Carter, E. A. *Phys Rev B* 2004, 69, 125109.
- Zhou, B.; Wang, Y. A. *J Chem Phys* 2006, 124, 081107.
- Roothaan, C. C. J. *Rev Mod Phys* 1951, 23, 69. Appendix I.
- Dunlap, B. I.; Connolly, J. W. D.; Sabin, J. R. *J Chem Phys* 1979, 71, 3396.
- Ingamells, V. E.; Handy, N. C. *Chem Phys Lett* 1996, 248, 373.
- Soler, J. M.; Artacho, E.; Gale, J. D.; García, A.; Junquera, J.; Ordejón, P.; Sánchez-Portal, D. *J Phys Condens Matter* 2002, 14, 2745.
- Perdew, J. P.; Zunger, A. *Phys Rev B* 1981, 23, 5048.
- Wang, Y. A.; Govind, N.; Carter, E. A. *Phys Rev B* 1999, 60, 16350; Erratum: *Phy Rev B* 2001, 64, 089903.
- Gonze, X.; Beuken, J.-M.; Caracas, R.; Detraux, F.; Fuchs, M.; Rignanese, G.-M.; Sindic, L.; Verstraete, M.; Zerah, G.; Jollet, F.; Torrent, M.; Roy, A.; Mikami, M.; Ghosez, P.; Raty, J.-Y.; Allan, D. C. *Comput Mat Sci* 2002, 25, 478.
- Troullier, N.; Martins, J. L. *Phys Rev B* 1991, 43, 1993.
- Monkhorst, H. J.; Pack, J. D. *Phys Rev B* 1976, 13, 5188.